HYDROGEN JET STRUCTURE IN PRESENCE OF FORCED CO-, COUNTER- AND CROSS-FLOW VENTILATION

Grune, J. [1], Sempert, K. [1], Kuznetsov, M[2]. and Jordan, T.[2]
[1]Pro-Science GmbH, Parkstrasse 9, Ettlingen, 76275, Germany,
[2]Karlsruhe Institute of Technology, Kaiserstrasse 12, Karlsruhe, 76131, Germany

**Corresponding author: grune@pro-science.de*

ABSTRACT

This paper presents results of experimental investigations on unignited horizontal hydrogen jets in air in presence of co-, cross- and counter-flow. Hydrogen concentration distributions are obtained as functions of distance to the hydrogen release nozzle. The H_2-jet variables are two nozzle diameters, 1 mm and 4 mm and two H_2-jet mass flow rates, 1 g/s up to 5 g/s. A propeller fan is used to provide forced ventilation, compared to the case with no ventilation three different airflow velocities up to 5 m/s were studied systematically. It was found that any forced ventilation in co-, cross- and counter-flow direction reduces the size of the burnable mixture cloud of the H_2-jet compared to a free jet in quiescent air.

1.0 INTRODUCTION

Many hydrogen fuelled engines commonly use compressed hydrogen. Accidental hydrogen release from pipe systems or fuel tanks is one of the main hazards that occur in the handling of pressurized hydrogen. If initially the release of pressurised H_2 is unignited there is still a possibility that it will be ignited, after a certain delay, if an ignition source is present in the path of the release. Wind in the free field or forced ventilation in confined or semi-confined areas, like tunnels or parking garages, can become an influence of the H_2-dispersion. The release of pressurised H_2 and its dispersion was extensively studied, both experimental and theoretically [1-2]. The flow velocity, hydrogen distribution and scaling characteristics for high momentum hydrogen jets are consistent with the well-known scale correlations based on papers [3-6]. The axial hydrogen concentrations C(x) and the corresponding flow velocity u(x) on the jet axis can be written as a function of the distance x on the centerline of the jet axis:

$$\mathrm{C(x)} = C_0 \cdot A \cdot \frac{d_o}{(x + x_0)} \qquad (1) \qquad\qquad \mathrm{u(x)} = u_0 \cdot B \cdot \frac{d_o}{(x + x_0)} \left(\frac{\rho_{H2}}{\rho_o}\right)^{1/2} \qquad (2)$$

where A and B are empirical constants; C_0 and u_0 are the initial hydrogen concentration and flow velocity; d_0 is the original nozzle diameter; x_0 is a virtual origin displacement; ρ_o and ρ_{H2} are the densities of ambient air and hydrogen at the release point. From the practical point of view especially in case to describe safety distances of pressurised hydrogen release in air under the spectrum of natural ambient atmospheric conditions, in order to estimate how far from the release point a burnable H_2/air mixture is expected. Eq. (1, 2) can be simplified to express the axial hydrogen concentrations C(x) and flow velocity u(x) versus distance x to the release point:

$$\mathrm{C(x)} = A \cdot \frac{d_o}{(x)} (\dot{m})^{1/2} \qquad (3) \qquad\qquad \mathrm{u(x)} = B \cdot \frac{d_o}{(x)} (\dot{m})^{1/2} \qquad (4)$$

where A and B are empirical constants; $\dot{m}$ is the H_2-massflow rate per nozzle area. The H_2-massflow rate can be constant because controlled from the H_2-engine, or transient as blowdown of a pressurized H_2 reservoir like a tank or pipeline [7]. Nevertheless, the H_2-massflow rate per nozzle area in Eq. (3, 4) can be replaced by the overpressure P of the released gas near the nozzle. Due to the jet expansion and shear layer with entrainment of air the radial flow velocity and hydrogen concentration have a decaying radial profile

from centerline to edges of the jet. The hydrogen concentration and flow velocity have normal distribution across the flow, which can be described well by a Gauss function [6]:

$$C(r) = \frac{G1(x)}{G2(x)\sqrt{2\pi}} exp\left(-\frac{r^2}{2 \cdot G2(x)^2}\right) \quad (5) \qquad u(r) = \frac{G3(x)}{G2(x)\sqrt{2\pi}} exp\left(-\frac{r^2}{2 \cdot G2(x)^2}\right) \quad (6)$$

where r is the radial distance from the jet axis; G1(x), G2 (x) and G3 (x) are factors of the Gauss function. The term G1/ $((2(G2))^{1/2})$ is equal to the maximum local hydrogen concentration C(x)max on the jet axis (r = 0) and G3/$((2(G2))^{1/2})$ is the maximum flow velocity at the distance x on the jet axis. Due to the self-similar structure of the momentum dominated jet all the velocity and concentration radial profiles normalized by the centerline values $C(x)_{max}$ and $u(x)_{max}$ will collapse to one line against dimensionless radius normalized by half-width $r_{1/2}$ of the profile [6]. With the knowledge of axial H_2-concentrations C(x) and flow velocity u(x) in a distance x to the release point (Eq. 3; 4) and the knowledge of the factors G1(x), G2 (x) and G3 (x) (Eq. 5) depending on axial distance (x), hydrogen concentration and velocity distribution for the high momentum H_2-jet can be described in axial and radial direction. From the H_2-concentrations-field, the structure of the flammable cloud is determined.

The continuous release of pressurised H_2 into stagnant air is a kind of ventilation itself, a relatively small amount of H_2 with high velocity accelerates a relatively large amount of air during the mixing process. Due to this effect, a flow field is established in the environment of the release. However, the release of pressurised H_2 into still air is well understood while there is a lack of knowledge of the H_2-jet behaviours in the presence of forced ventilation. In literature, some investigations of cross-flow influence are available [8,9], regarding co- and counter-flow only recent publications from burner development are present [10].

The goal of the work is an experimental investigation of the hydrogen jet structure and its dispersion in the presence of co-, cross- and counter-flow to characterize the hazard distances as a function of the ratio of hydrogen mass flow rate and airflow velocity of the forced ventilation. Therefore experiments were performed with H_2-jets for two nozzle diameters (1 mm and 4 mm) and two hydrogen mass flow rates (1 and 5g/s). A propeller fan was used to provide forced ventilation, compared to the case with no ventilation three different airflow velocity's 1.5 m/s, 3.5 m/s and 5 m/s were studied systematically. The main topic is a database for numerical simulation [11] to provide unique experimental data for numerical model development and validation and contribution to the recommendations for inherently safer use of hydrogen vehicles in underground transportation systems and other confined or semi-confined areas.

2.0 EXPERIMENTAL SET-UP

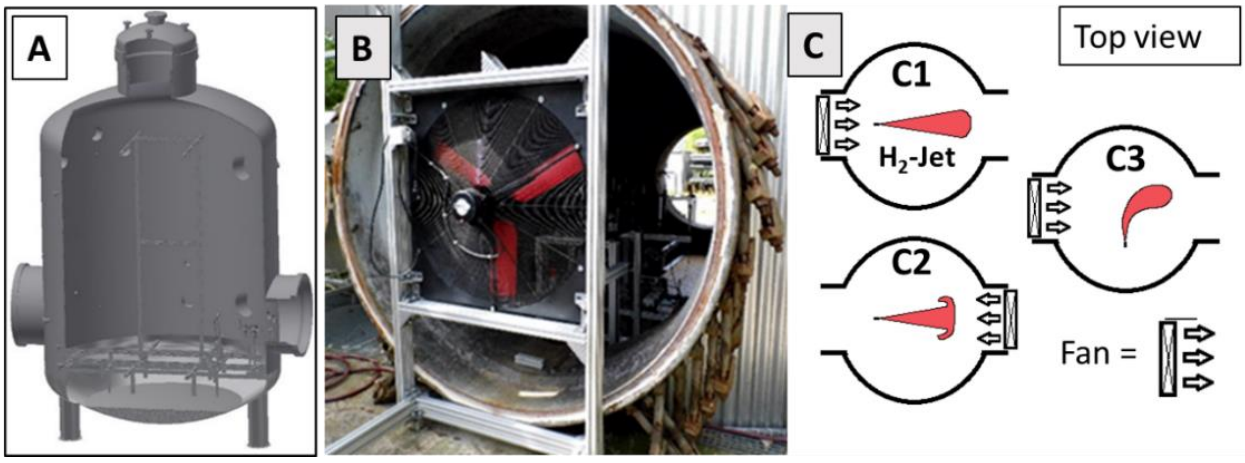

Figure 1: A) 220 m^3 test vessel with two parallel flange doors. B) Propeller fan placed on a flange door. C) Top view sketches of the H_2-release for three different ventilation configurations: co-flow (C1), counter-flow (C2) and cross-flow (C3).

The experiments were performed at the KIT hydrogen test site HYKA in a 220 m^3 test vessel. The test vessel Fig. 1A is equipped in the upper part with two large parallel flange doors (d = 1.8 m). On one of these flange doors a propeller fan was placed to provide forced ventilation between the two flange doors, Fig. 1B. The pivot point of the fan and the H_2-release nozzle are axially centered with the flange doors. The sketch Fig. 1C right shows the top view of the test vessel with the position of the fan and the release direction of the H_2-jet. The H_2-jet position is identical for the co-flow (C1) and counter-flow (C2) configuration only the position of the fan is changed from one flange door to the opposite one. For the cross-flow (C3) configuration, the position of the H_2-release was set to be perpendicular between the two flange doors. All experiments were performed with fully open flange doors. In the experiments without forced ventilation, the fan was removed from safety vessel A2. Fig. 2 left shows the scheme of the H_2-jet facility. The H_2-mass flow rate was adjusted via a needle valve and a Coriolis device. A long pipeline (length > 15 m; di = 4 mm) is used to transport the H_2-flow close to the release nozzle. In the start-up of the H_2-flow adjustment the H_2-flow runs first in a bypass line with an installed nozzle copy of the release nozzle. By synchronous closing and opening of the bypass and release valve the H2-jet can be established and switched off fast. The release nozzle is lifted up from the valves to prevent the blocking and additionally turbulence of the forced ventilation in co-flow configuration.

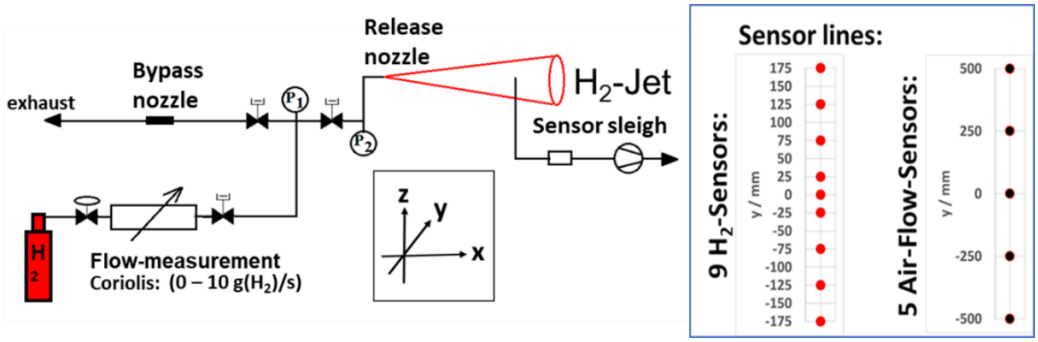

Figure 2: Left, schema of the H_2-jet facility. Right, positions in y-directions of the sensors (H_2-concentration and airflow) on the sensor sleigh.

Fig. 3 left shows the dependency between the adjusted H_2-mass flow rates for different nozzle sizes (pre-test and main test) and the measured pressure P2 close to the nozzle. The diagram shows a linear dependency between the flow-rates, expressed as flow-rate per nozzle area, and the measured pressure in the pipeline (di = 4 mm) near the nozzle exit. The H_2-concentration in the free-jet cloud was measured with nine independent thermal conductivity sensors connected to a small laboratory pump. Therefore a fixed sensor line, Fig. 2 right, consisting of nine 600 mm long pipelines (di = 2 mm) used to place the sample points horizontal and perpendicular to the jet-axis. In each test, the sensor-line was fixed in one x position and measured simultaneous nine H_2-concentration points in y–direction without disturbing the jet-structure in the axial direction.

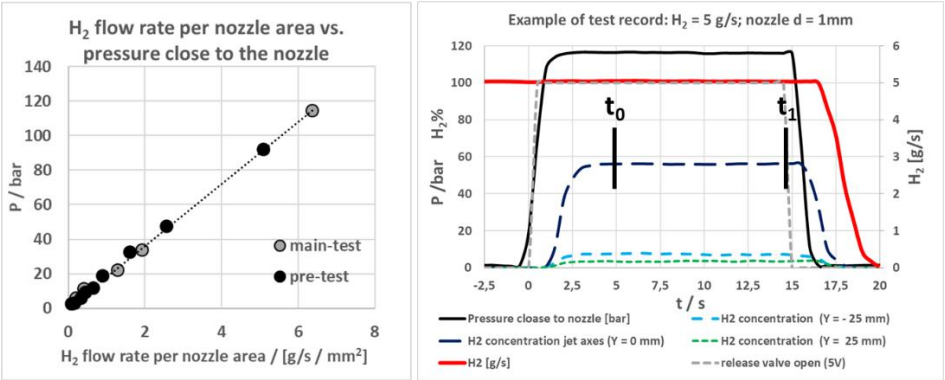

Figure 3:Dependency of the measured pressure P2 near to the nozzle against H_2-mass flow rates per nozzle area (left). An example of a test pressure record (right)

The sensor line sleigh can be shifted up to an axial distance to the nozzle of x = 3500 mm. The measured values were recorded with a sample rate of 2 Hz. Fig. 3 (right) shows exemplary pressure-time history at the distance to the nozzle x = 125 mm for 1 mm nozzle and a flow rate of 5 g/s H_2. In the startup (t < 0), the flow-rate is adjusted and established through the bypass. At t = 0, the release valve opens and the bypass valve closes synchronous, no disturbance of the flow rate of 5 g/s H_2 is visible. By switching the valve the pressure near the nozzle exit rises to a constant value (117 bar) and the H_2-jet with a constant flow-rate is established in the test area. The first signal from the H_2-sensors is recorded 1 s after the H_2-release was initiated. A constant value of mass flow rate is reached after 5 s release time. Steady state conditions can be assumed in a time span of 10 s between t_0 and t_1, Fig. 3 right. In experiments with 1 g/s H_2-release rate the time span between t_0 and t_1 was 25 s. As a result of the concentration measurement, the average concentration between the time t_0 and t_1 will be stated. Additional information on turbulence is given by the maximum and minimum values in this time frame of steady state conditions.

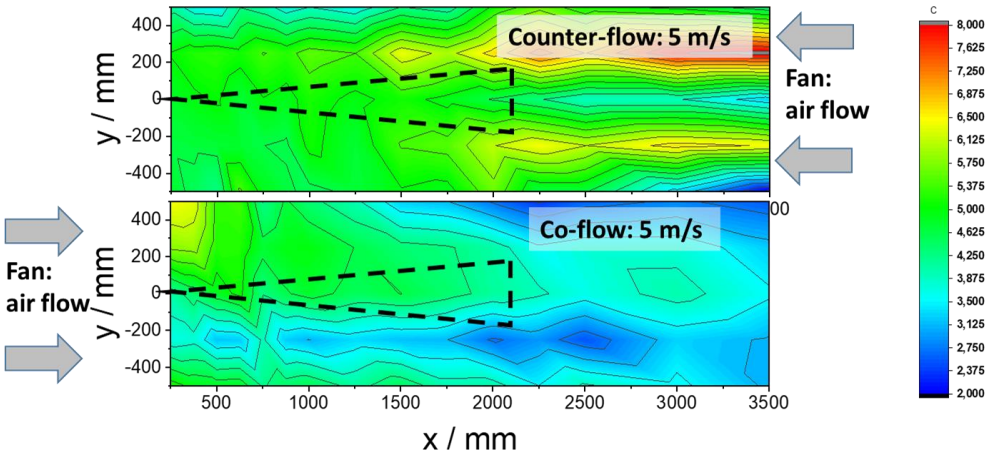

Figure 4: Contour plots of flow velocities in x-direction for counter- and co-flow configurations for 5 m/s of airflow velocity. Color scale (right) is the velocity in m/s.

To realize a forced ventilation a propeller fan was used, Fig. 1B. The fan has a maximum airflow of 20000 m^3/h and the maximum declared flow velocity of 8.8 m/s. The maximum produced air overpressure is 110 Pa and the propeller diameter is 920 mm. The position of the fan for the investigated configurations is shown in Fig. 1 C. The flow velocities in x-direction were measured in the horizontal x-y-area using a sensor line with five airflow sensors, Fig 1 right. Therefore, the airflow velocity was recorded for a duration of 1 min with a frequency of 2 Hz. Fig. 4 shows contour plots of the average flow velocities in the x-direction for counter- and co-flow configuration (5 m/s) for the horizontal x-y-area.

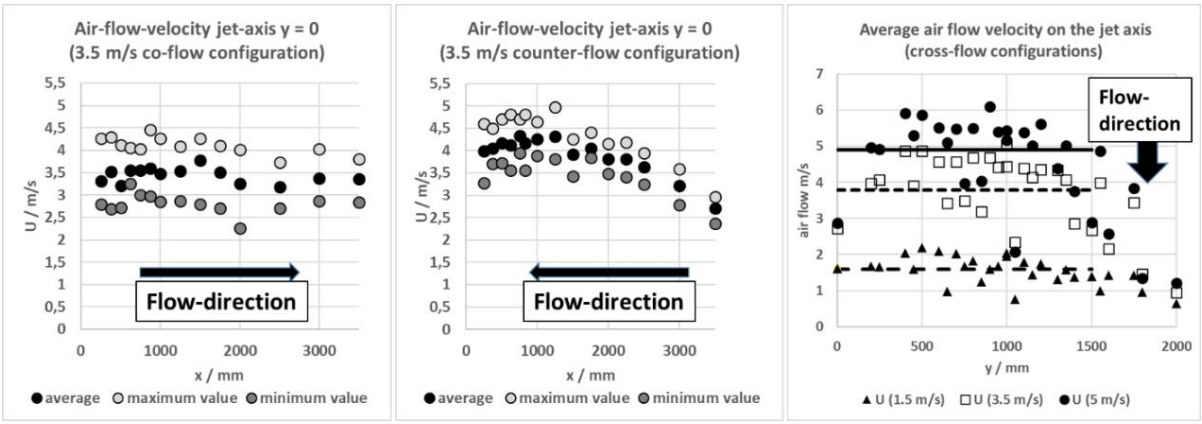

Figure 5: Co- and counter-flow velocities in x direction along the x axis for 3.5 m/s air flow (left and middle). Airflow velocities in x direction along the y axis for velocities 1.5, 3.5 and 5 m/s for cross-flow.

The flow velocity in the contour plots shows a passable agreement with the adjusted value of 5 m/s for both opposed directions in the x-y area of the H_2-jet. The produced flow field from a propeller fan is highly turbulent. Figs. 5 (left and middle) show the airflow velocities along the x-axis for the 3.5 m/s layout for co- and counter-flow. The average maximum and minimum velocities for 1 min time window are plotted. The variability is sometimes more than +/- 1 m/s. In the counter-flow case the airflow velocities in the center near the fan, x > 2500 mm, are remarkable low. This effect is typical for a propeller fan and can be observed in detail in Fig.4 top, low velocity on the fan hub position (y = 0) and high velocity near the maximum radius of the propeller (y = +/- 300 mm). Nevertheless, in the x-y area, within 0 < x < 3500 mm, the flow velocities in x-direction are in a passable agreement with 3.5 m/s for both opposed directions. The useable airflow field in the cross-flow case, where the airflow is perpendicular to the H_2-jet axis, is limited to the size of the fan. Fig. 5 right shows the average airflow velocities in x direction along the y-axis for 1.5 m/s, 3.5 m/s and 5 m/s configuration for the cross-flow case. In a distance y > 1500 mm the airflow velocities (3.5 m/s and 5 m/s layouts) significantly decay.

3.0 RESULTS

Table 1 shows the 40 different investigated configurations. The variables are two nozzle diameters (1 mm and 4 mm) two H_2-mass flow rates (1 g/s and 5 g/s) and four airflow velocities (0 m/s; 1.5 m/s; 3.5 m/s and 5 m/s). In the cross-flow case, the high H_2-mass flow rate of 5 g/s is replaced to 1.5 g/s for the 1 mm nozzle and 2.5 g/s for the 4 mm nozzle since the size of the airflow field is limited for this configuration. In more than 600 release experiments, the H_2-concentration for all configurations was measured systematically in the horizontal x- y-domain of the jets.

Table 1: Test Matrix

H_2 mass-flow rate/ g/s	Nozzle diameter/ mm	Stagnant	Co-flow/ m/s	Counter-flow m/s	Cross-flow m/s
1	1; 4	0	1.5; 3.5; 5	1.5; 3.5; 5	1.5; 3.5; 5
1.5	1				1.5; 3.5; 5
2.5	4			1.5; 3.5; 5	1.5; 3.5; 5
5	1; 4	0	1.5; 3.5; 5		

The influence of forced ventilation on the H_2-jet structure will be investigated by comparison with no ventilation case. Fig. 6 shows the H_2-concentration on the jet axis (Y = 0) for all configurations without forced ventilation. The points of the reciprocal H_2-concentration vs. normalized distance from the nozzle, according to (Eq.3), collapse for all configurations to the same linear dependency. Alternatively, the release overpressure P can be expressed by the H_2-mass flow rates per nozzle area, Fig 3 left.

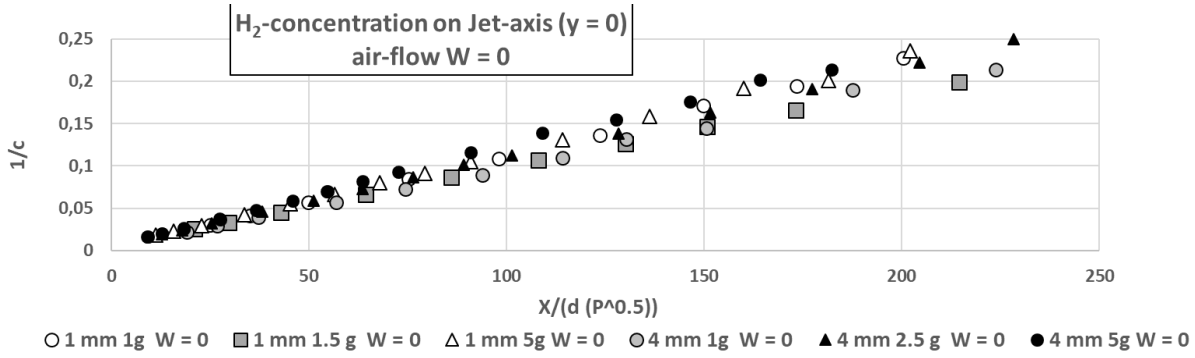

Figure 6: Reciprocal H_2-concentration on the jet axis vs. normalized distance from the nozzle for all configurations with H_2-release into stagnant air. (c in vol.% H_2; x in mm, d in mm; P in bar).

3.1. Co- and Counter-flow

The influence of a forced co- and counter flow ventilation on the H_2-concentration on the jet axis (Y = 0) is shown in Fig. 7. For the cases with co- and counter-flow ventilation, the reciprocal

H_2-concentration vs. normalized distance from the nozzle deviates from the linear character. Near the nozzle exit, the H_2-concentrations for cases without and with co- or counter-flow ventilation are equal. After some distance where the velocity in hydrogen jet is comparable with airflow velocity, the H_2-concentration starts to decay faster for the forced ventilated cases. It is seen that the influence of a ventilation velocity of 1.5 m/s is nearly negligible for the H_2-concentration on the jet axis, independent of co- or counter-flow direction. The only exception is the release case with the lowest jet impulse (nozzle d = 4 mm; H_2 mass flow = 1 g/s), the co-flow case (airflow 1.5 m/s) shows a strong deviation compared to the case without ventilation. For the higher ventilation velocities (airflow 3.5 m/s and 5 m/s) all cases show from a certain distance point a strong deviation from the straight dependencies observed for the cases with no ventilation. The lower the impulse amount of the released H_2 the stronger the concentration decay along the jet axis.

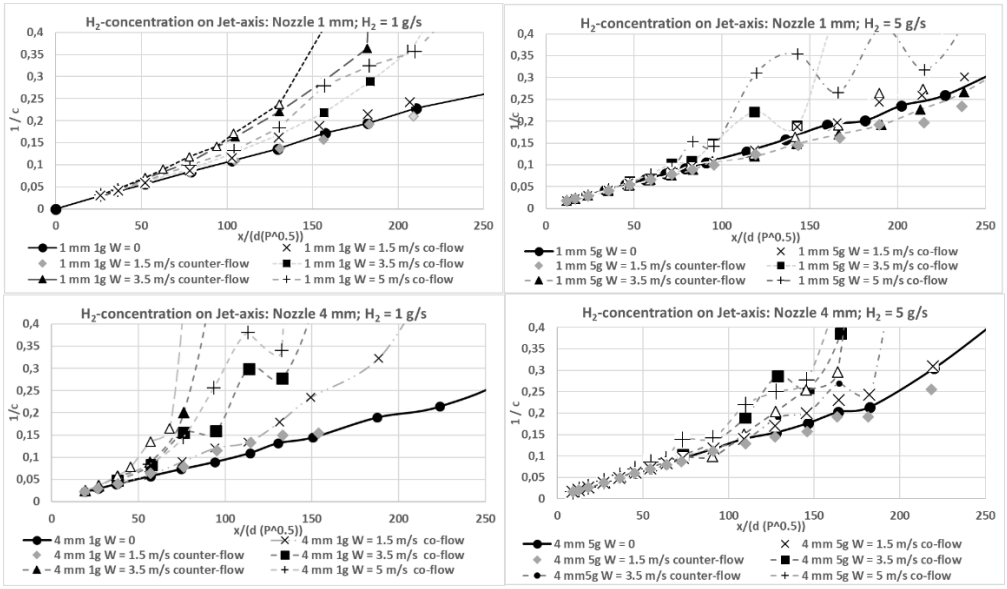

Figure 7: Reciprocal H_2-concentration on the jet axis vs. normalized distance from the nozzle for co- and counter-flow layout compared to H_2-release in stagnant air. (c in vol.% H_2; x in mm, d in mm; P in bar).

Fig. 8 demonstrates the quantity of H_2-concentration measurement points in the investigated horizontal x, y-domain. The figure shows exemplarily the H_2-concentration along the y-axis for different distances x to the nozzle. Clearly visible is the symmetrical Gaussian H_2-concentration profile along the y-axis, as also the rapid H_2-concentration decaying along the x-axis for the points (y = 0) on the jet-axis. With this amount of concentration points it is possible to create contour plots of the H_2-concentration distribution in the investigated x, y-domain to compare the cases with and without forced ventilation. All presented H_2-concentration contour plots show the stated average H_2-concentration (Fig.3).

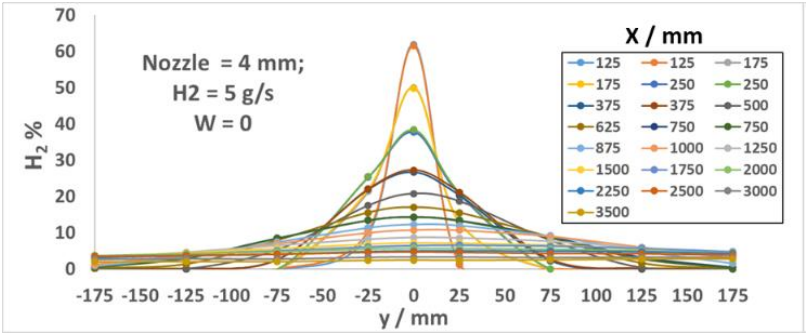

Figure 8: Radial H_2-concentration profiles for different distances x to the nozzle. (Nozzle d = 4 mm; H_2 = 5 g/s; no ventilation W = 0)

Fig. 9 shows contour plots for the 1 mm nozzle and a constant H_2-release rate of 1 g/s to compare the influence of the H_2-concentration distribution for different co- and counter-flow ventilations. As a reference, the H_2-concentration surface of a release in stagnant air (W = 0) is shown. Below, on the left side, the H_2-concentration surface with counter-flow ventilations and on the right side, the co-flow ventilations are stacked. The colored H_2-concentration scale covers flammable concentrations in the range from 4 % H_2 (dark blue) up to 32 % H_2 (dark red). For the configuration (nozzle = 1 mm; H_2 = 1 g/s), the tip of the 4 % H_2 limit spreads to a distance of 1.2 m without ventilation. For a lower ventilation velocity of 1.5 m/s the level of 4 % H_2 spreads to the same axial distance of 1.2 m for counter-flow direction while in co-flow direction a remarkable reduction of the 4 % H_2 limit spread is observed. With increasing ventilation velocity (3.5 m/s and 5 m/s) the 4 % H_2 limit distances were reduced for both opposite ventilation directions. In general, it demonstrates a hyperbolic dependence of burnable cloud dimension against ventilation velocity. The burnable mixture cloud with co-flow ventilation shows a narrower shape in contrast to the jets with counter-flow ventilation. These two results regarding the size and shape of hydrogen cloud are the major findings for safety measures.

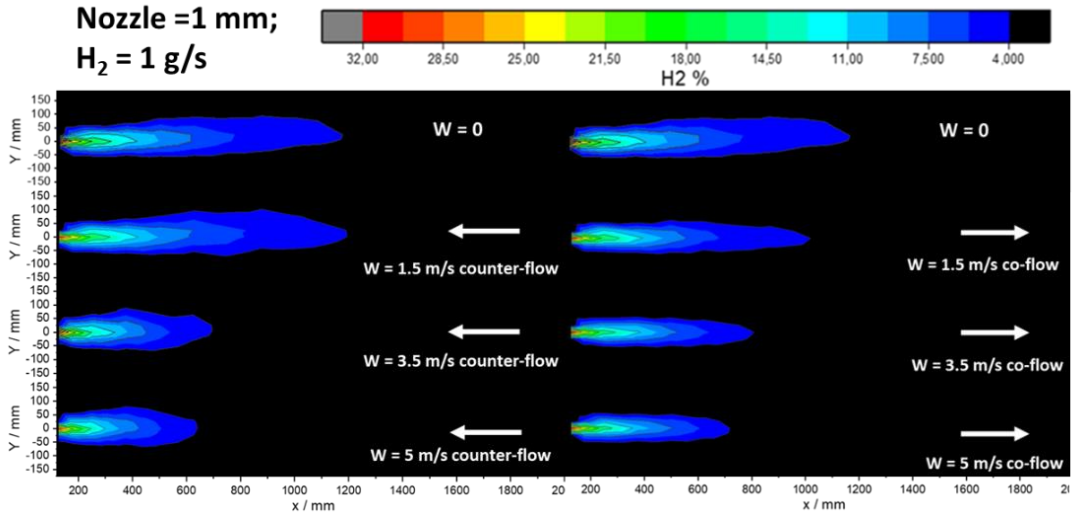

Figure 9: Hydrogen - contours for 1 mm nozzle and H_2-release rate of 1 g/s. Color scale is in vol. %H_2.

Fig. 10 shows that for a higher H_2-release rate (5 g/s) the general behavior is the same as in Fig. 9. There is no influence of the jet structure with a low ventilation velocity (1.5 m/s) in counter-flow direction compared to the jet shape without ventilation. With increasing flow-velocity the distance of the 4 % H_2 limit decreases for both opposite ventilation directions. However, the reduction of the burnable mixture cloud is more pronounced for ventilation in co-flow direction. The effect of the different shape structures of the H_2-dispersion for co- and counter-flow ventilation affects mainly H_2-concentrations nearly or below the flammability limit, within a domain of lower local flow velocity of the jet.

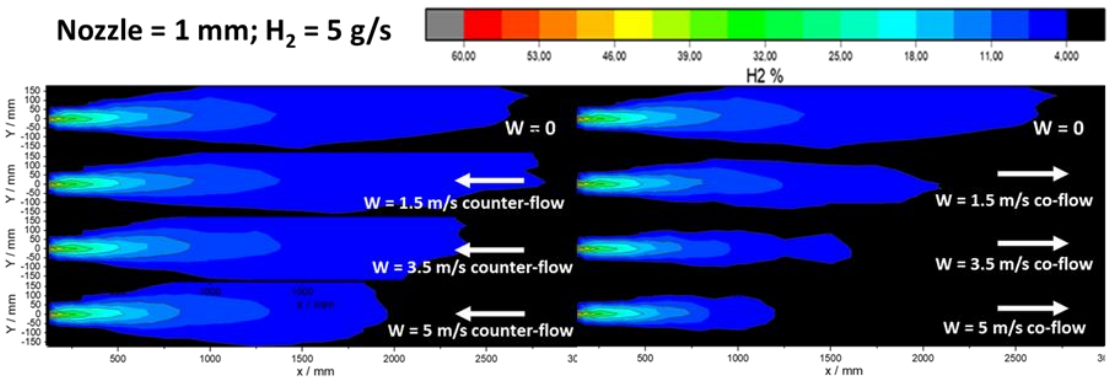

Figure 10: Hydrogen - contours for 1 mm nozzle and H_2-release rate of 5 g/s. Color scale is in vol. %H_2..

Fig. 11 shows contour plots that highlight the non-burnable H_2-concentration between 0.1 % and 3.9 % H_2 for 1 mm nozzle and constant H_2-release rate of 1 g/s with 5 m/s co-flow and counter-flow ventilation velocity. With forced co-flow ventilation the lean mixture spreads in flow direction with very smooth concentration decay, while in the counter-flow ventilation case the concentration decays within a short distance. The forced counter-flow ventilation completely changes the initial H_2-jet flow direction from some point and the lean mixture cloud follows the ventilation direction. This effect leads to a wider shape of the H_2-dispersion in case of forced counter-flow ventilation. The H_2-dispersion for lean mixture domains, near the flammability limit, is very different for co- and counter-flow ventilation. Regardless of this, the spread of the 4 % H_2 limit distance is sometimes equal for both opposite ventilation flow directions.

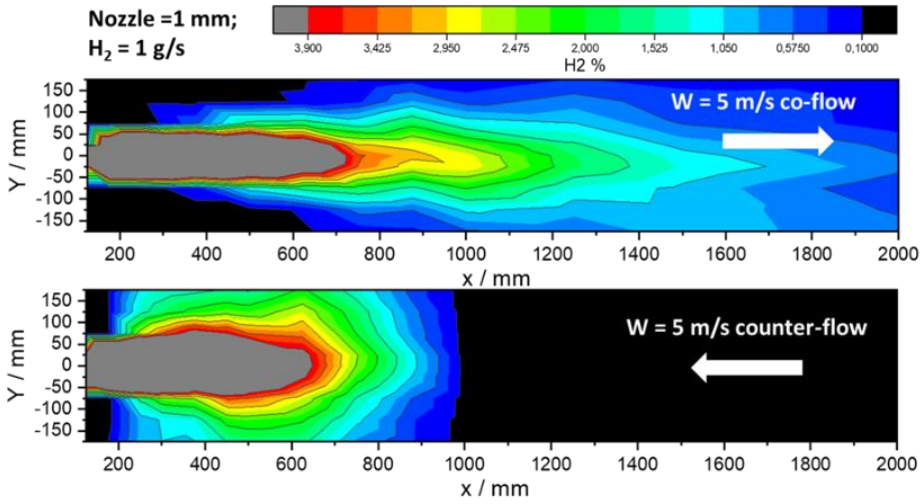

Figure 11: *Contour plots (Non-burnable H_2-concentration 0.1 % to 3.9%) for the 1 mm nozzle and a constant H_2-release rate of 1 g/s. Top, 5 m/s co-flow ventilation. Down 5 m/s counter-flow ventilation*

Fig. 12 left shows contour plots for the 4 mm nozzle and a constant H_2-release rate of 5 g/s to compare the influence of the H_2-concentration distribution for 5 m/s co- and counter-flow ventilations. The axial distance reduction for the 4 % H_2 limit distance appears to be the same for both ventilations cases. For the H_2-release in stagnant air, the 4 % H_2 limit distance lies at 2.75 m while with 5 m/s co- and counter-flow ventilations this distance is reduced to 2 m. Indeed, only the low-velocity part of the jet with the relative lean mixture is involved. Fig. 12 right shows the same H_2-releases as Fig. 12 left with different concentration scales. In this contour plot, the reactive concentration range within the range of 15–35 % H_2 is highlighted. It is visible that the differences between the three varied cases become much smaller because of the region of high velocity which is not affected by the ventilation flow. Due to the similarity of concentration and velocity profiles, we conclude that the higher the concentration and local velocity in the jet, the less influence of forced ventilation is observed. For H_2-concentration above 20 %H_2 the effect of ventilation looks negligible.

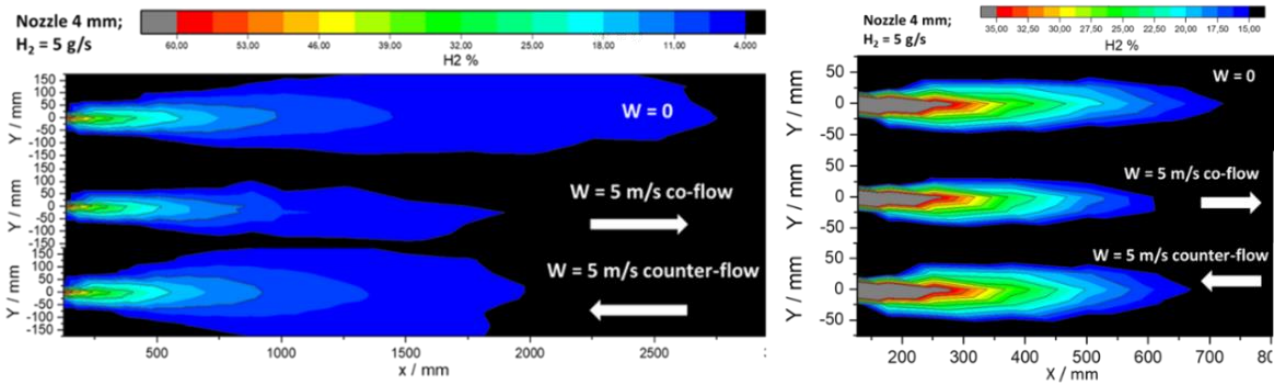

Figure 12: Contour plots for the 4 mm nozzle and a constant H_2-release rate of 5 g/s. Left, concentration range between 4 % and 60 % H_2. Right, concentration range between 15 % and 35 % H_2 range.

3.2 Cross-Flow

In the cases of co-and counter flow configurations, the influence of the forced ventilation is symmetrical to the H_2-jet axis. A forced cross-flow ventilation destroys the symmetry with respect to the jet axis. Fig. 13 right top shows exemplarily the radial H_2-concentration profiles for different distances x to the nozzle in the case of no ventilation (nozzle d = 4 mm; $\dot{m}$ = 2.5 g/s; W = 0). Fig. 13 right down shows the same H_2-release in presence of cross-flow ventilation of 5 m/s. It leads to the shift of the tail of low concentrations in a wind direction, fully destroying the symmetry of the Gaussian profile as in stagnant air conditions. The only kernel of the H_2-concentration profile in a near distance to the nozzle remains unchanged in this case.

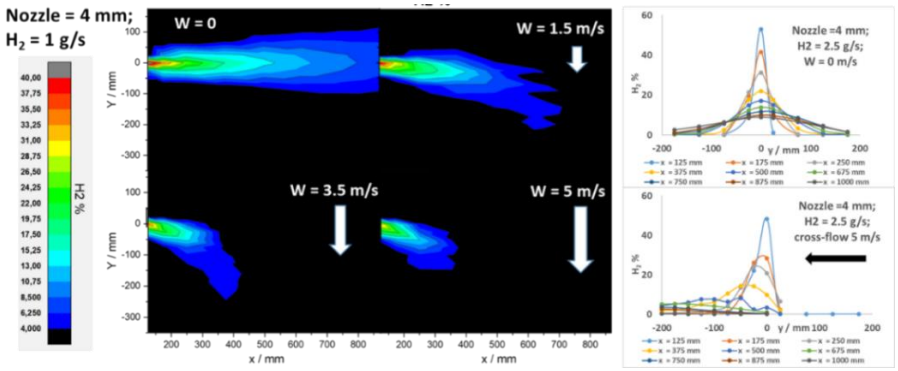

Figure 13: H2 - contour (d_0 = 4 mm, $\dot{m}$ = 1 g/s) for different cross-flow ventilations (left). Radial H_2-concentration profiles at different distances to the nozzle x (d = 4 mm; $\dot{m}$ = 2.5 g/s) with cross-flow ventilation (W=5 m/s) and without (W = 0), right.

Fig. 13 left shows contour plots for the 4 mm nozzle and H_2-release rate of 1 g/s to compare the influence of the H_2-concentration distribution for different cross-flow ventilation. It is compared with the H_2-concentration profile of the release in stagnant air (Fig. 13 top left, W = 0). Aside and below the H_2-concentration structure of releases with the three investigated cross-flow ventilation velocities of 1.5, 3.5 and 5 m/s are shown. The colored H_2-concentration scale covers the range from 4 % H_2 (dark blue) to 40 % H_2 (dark red). It is visible that the area of the burnable mixture cloud is strongly reduced with increasing of the cross-flow ventilation impact on the H_2-jet. For this configuration (d = 4 mm; H_2 = 1 g/s) the tip of the 4 % H_2 limit spreads to a distance of 1.64 m without ventilation. The diagonal of the x/y distances of the tip with 4 % H_2 used to compare the cases with cross-flow with release in stagnant air. This will be discussed in the next chapter.

3.3 Reduction of Safety Distance due to the Ventilation

The safety distance can be defined, as the distance to the nozzle where the H_2-cloud is not ignitable (beyond the 4 % H_2 limit). It was observed that the impact of forced ventilation on the investigated H_2-releases leads to a reduction of the safety distance. The only exception is the case of counter-flow ventilation with a low airflow velocity of 1.5 m/s. Fig. 14 summarizes the influence of ventilation on the safety distances for the investigated cases. Therefore, the measured safety distances for all H_2-jets without ventilation are normalized to compare this normalized distance with the corresponding safety distance from H_2-releases with forced ventilation. These plots show the normalized safety distances against the ventilation velocity for three directions of the ventilation flow. Fig. 14 left shows the influence of co-flow ventilation on the safety distance. In this case, a ventilation flow velocity of 1.5 m/s leads to a 20% lower safety distance. For a co-flow velocity of 5 m/s the safety distance is reduced by 40 % to 60 %, compared to the case without ventilation. For the counter-flow case (Fig. 14 center), the only case with the lowest impulse (nozzle d = 4 mm; H_2 = 1 g/s) shows nearly the same reduction of the safety distance as the co-flow case. All others show an insignificant increase (1 % to 4 %) of the safety distance in the case of a low ventilation velocity of 1.5 m/s. For higher counter-flow velocities the safety distance significantly decreases. For 3.5 m/s it reduces by 40 % and for 5 m/s the safety distance is reduced by 30% to 65 %. The highest reduction of safety distances was observed for the cross-flow configuration, where the ventilation impact is perpendicular to

the H_2-jet axis. In this case, the safety distances were extracted as diagonal of the x/y distances of the tip with 4 % H_2. Fig. 14 right shows the normalized reduction of the safety distance for the cross-flow configuration. The lowest studied airflow velocity of 1.5 m/s leads to a remarkable reduction of the safety distance between 38 % and 60 %. With increasing cross-flow ventilation velocity, the normalized safety distance also decreases. For a cross-flow velocity of 5 m/s the observed reduction of the safety distance is between 65 % and 80 %, compared to the case without ventilation.

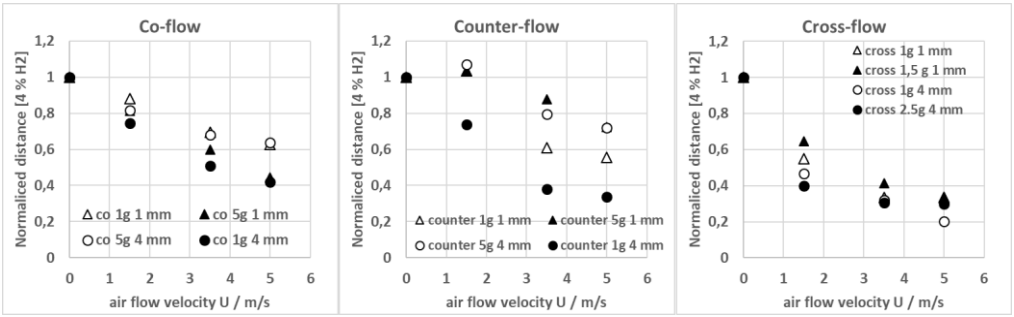

Figure 14: The influence of ventilation on normalized safety distances for co-, counter- and cross-flow.

4.0 DISCUSSION

The continuous and constant release of pressurised H_2 into stagnant air and its dispersion leads to the formation of the steady state H_2/air cloud and can be monitored by the measured concentrations and velocities. Hydrogen jet flow expands and mix with entrained air with formation of the similar H_2-concentration and flow velocity profiles. Both profiles are characterized by hyperbolic decay of the velocity and H_2-concentration in accordance with Eq. 1, 2. The shape of the radial flow velocity and hydrogen concentration profile can be described well by the Gauss function (Eq. 5, 6). Thanks to a sufficient amount of concentration measurement points, it was possible to create a normalized Gauss fit of the concentration profiles in a wide range of axial distances of the jets to evaluate the Gaussian factors G1 and G2 in Eq. 5.

Fig. 15 top left shows normalized Gaussian functions and the experimental concentration measurement points for different axial distances for H_2-release case (d = 4 mm; H_2 = 5 g/s). The generated normalized Gaussian factors G1 and G2 both show a linear dependence regarding the distance x to the nozzle. The values of G1 and G2 increase with axial distance x increase, Fig. 15 top right. Amazingly, the normalized Gauss coefficient of the concentration profiles from all investigated H_2-release cases leads to the same linear slope along with the axial jet distance. Fig. 15 top right shows all axial linear fits of the normalized Gaussian factors G1 and G2. With the knowledge of the maximum concentration on the jet axis (Fig.6) and the normalized Gaussian factors G1(x) and G2(x) for all positions on the jet axis the concentration distribution of an axis symmetrical free H_2-jet is linked with a simple correlation in full H_2-jet range. A normalized Gauss fit of the concentration profiles from the measured concentration data in case of forced ventilation is only for the co-flow configuration possible. Fig. 15 top down shows exemplary the gained normalized Gaussian function factors G1(x) and G2(x) over the axial distance for the H_2-release case, d = 4 mm; H_2 = 5 g/s, co-flow W=5m/s. Additionally, it is plotted the potential fit of factors G1(x) and G2(x) for all investigated H_2-release cases with co-flow ventilations of 5 m/s. The slope along the axial jet distance for G2(x) is very identical for all cases while the slope for G1(x) spreads a little more. Nevertheless, the main dependence, expressed as a potential fit, allows to define the Gaussian functions factors G1(x) and G2(x) as a function of the distance x for all investigated H_2-release cases with 5 m/s co-flow ventilation. By using the differences of the normalized Gaussian functions factors from the jet release in stagnant air (Fig. 15 top right) and the jet release with 5 m/s co-flow ventilation it is possible to plot a normalised radial concentration profile along the jet axis for co-flow ventilation. Fig. 15 left down shows the calculated normalised radial concentration profiles for different axial distances and co-flow conditions of 5 m/s. The normalization threshold is the maximum concentration on the jet axis of H_2-free jet into the stagnant air. The deviation of the maximum concentration from 1 reflects directly the faster decaying of the concentration in the case of a co-flow ventilation with 5 m/s as the release in stagnant air.

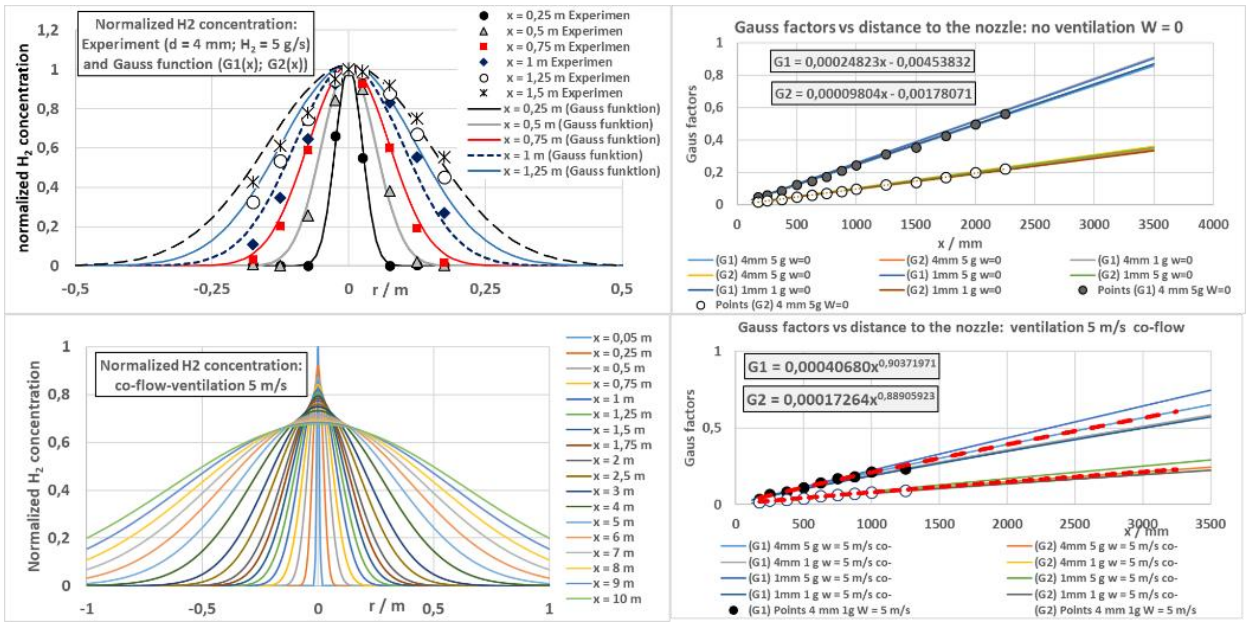

Figure 15: Left top, normalized Gaussian functions and the corresponding concentration measurement points for different axial distances (d = 4 mm; H_2 = 5 g/s). Right top, linear axial dependences of normalized Gaussian factors G1(x) and G2(x) no ventilation. Left down, calculated normalised radial concentration profiles for different axial distances and co-flow 5 m/s. Right down, non-linear axial dependences of normalized Gaussian factors G1(x) and G2(x) in case of co-flow ventilation (5 m/s).

With this method, the H_2-concentration field of similar pressurised H_2-release with round nozzles in still air can be recovered by using Eq. 3, with the function of the maximum concentration on the jet axis, (Fig. 6), and Eq. 5 with the normalized Gaussian coefficients G1(x) and G2(x) presented in Fig. 15 top right. The method is compatible to take the co-flow ventilation into the account by using special normalized Gaussian coefficients G1(x) and G2(x) as shows for 5 m/s co-flow velocity in Fig. 15 down right. Fig. 16 shows the results of this correlation. The left side shows the comparison with experimental results for the case: nozzle d = 4 mm, H_2 = 5 g/s, with no ventilation (W = 0) and co-flow ventilation W = 5 m/s. For both examples the 4 % H_2 limit is slightly over-predicted due to the turbulent diffuse border in the flow conditions near the 4 % H_2 limit, see Fig. 11. Fig. 16 right gives an impression on the H_2-concentration shape for constant 700 bar H_2-release with round nozzles of 1 mm in stagnant air and demonstrates the effect of co-flow ventilation with 5 m/s on this release conditions.

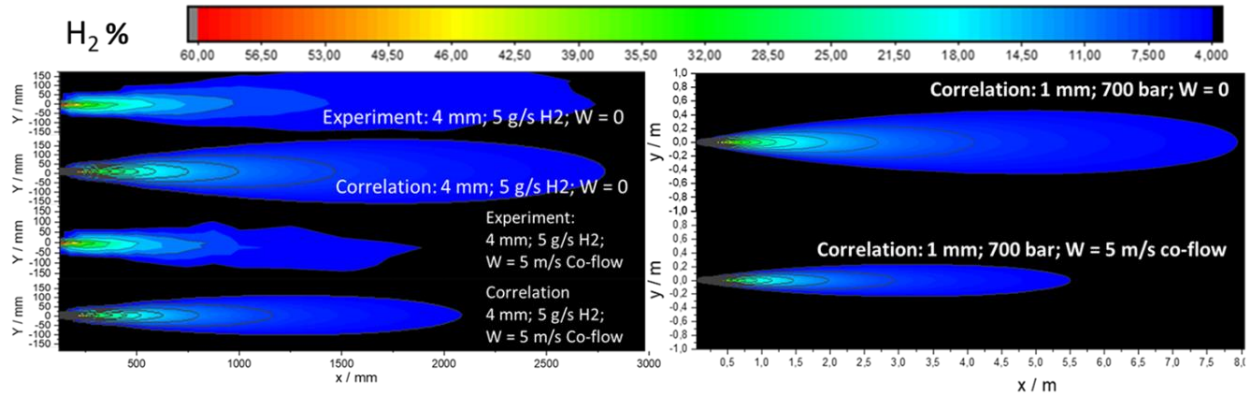

Figure 16: Left, comparison of correlation with experimental results, nozzle = 4 mm, H_2 = 5 g/s, with no ventilation (W = 0) and co-flow ventilation with 5 m/s. Right, correlation of the H_2-concentration shape 700 bar H_2-release nozzles 1 mm with no ventilation (W = 0) and co-flow ventilation with 5 m/s.

5.0 SUMMARY AND CONCLUSIONS

This work investigates H_2-jet structure in the presence of forced co-, counter- and cross-flow ventilation. The hydrogen concentration distribution is obtained as a function of distance to the release nozzle. The influence of ventilation and its direction on H_2-jet structure was expressed by the comparison with jets into stagnant air. It was found that forced ventilation reduces the size of the burnable mixture cloud (conventional safety distance beyond the 4 % H_2 flammability limit) for all H_2-jets compared to a free jet in stagnant air. Cross-flow ventilation leads to the strongest reduction of the safety distance and the H_2-jets are sensitive to low ventilation velocity (1.5 m/s). In few cases with low velocity counter-flow, a minor increase of the safety distance was observed. The general conclusion is that with increasing ventilation velocity the safety distance as 4 % H_2 limit decreases. Under the flow velocity of 5 m/s the safety distance is reduced by 65 % to 80 % for cross-flow, by 30 % to 65 % for counter-flow and by 40 % to 60 % for co-flow ventilations. Furthermore, a correlation model was presented to link the H_2-jet structures in stagnant air and in the presence of co-flow ventilation in a wide range of jet conditions.

ACKNOWLEDGMENTS

The authors are thankful to the Fuel Cells and Hydrogen Joint Undertaking (FCU JU) for the funding of HyTunnel-CS project (Grant agreement No 826193).

REFERENCES

1. Houf W, Schefer R. Analytical and experimental investigation of small-scale unintended releases of hydrogen. Int J Hydrogen Energy 2008;33:1435e44.
2. Chen CJ, Rodi W. Vertical turbulent buoyant jets: a review of experimental data. In: NASA STI/Recon Technical Report A80, 1980
3. Molkov, V., Bragin, M., Brennan, S., Makarov, D., Saffers, J.-B. (2010) Hydrogen safety engineering: Overview of recent progress and unresolved issues. International Congress Combustion and Fire Dynamics, Santander, Spain, 63-81
4. Birch AD, Brown DR, Dodson MG, Swaffield F. The structure and concentration decay of high pressure jets of natural gas. Comb Sci Tech 1984;36:249e61.
5. Birch AD, Hughes DJ, Waffield F. Velocity decay of high pressure jets. Comb Sci Tech 1986;52:161-71.
6. Veser, A. Kuznetsov, M. et al The structure and flame propagation regimes in turbulent hydrogen jets, International Journal of Hydrogen Energy Volume 36, Issue 3, February 2011, Pages 2351-2359 .ijhydene.2010.03.123
7. J. Grune, K. Sempert, M. Kuznetsov, W. Breitung Experimental study of ignited unsteady hydrogen jets into air International J Hydrogen Energy, 0360-3199, 36 (Issue 3) (February 2011), pp. 2497-2504, 10.1016/j.ijhydene.2010.04.152
8. Zhang, L., and Yang, V. (March 21, 2017). "Flow Dynamics and Mixing of a Transverse Jet in Crossflow—Part I: Steady Crossflow." ASME. *J. Eng. Gas Turbines Power*. August 2017; 139(8): 082601.
9. Ann R. Karagozian, The jet in crossflow, Phys. Fluids, 26(10): 101303 (2014)
10. Donghee Han, M.G. Mungal, Simultaneous measurements of velocity and CH distributions. Part 1: jet flames in co-flow, *Combustion and Flame*, 132(3) 2003, pages 565-590
11. S.G. Giannissi, I.C. Tolias, H. Ebne Abbasi, D. Makarov, J. Grune, K. Sempert, "Modelling of ventilated hydrogen dispersion in presence of co-flow and counter-flow ", ICHS2021, Edinburgh 21-23 September 2021.